

Analytical and computational study of magnetization switching in kinetic Ising systems with demagnetizing fields

Howard L. Richards

*Center for Materials Research and Technology,
(<http://www.martech.fsu.edu>)*

*Department of Physics,
(<http://www.physics.fsu.edu>)*

*and Supercomputer Computations Research Institute,
(<http://www.scri.fsu.edu>)*

Florida State University, Tallahassee, Florida 32306-3016

Department of Solid State Physics,

*Risø National Laboratory, DK-4000 Roskilde, Denmark
(<http://risul1.risoe.dk>)*

M. A. Novotny

Supercomputer Computations Research Institute,

Florida State University, Tallahassee, Florida 32306-4052

*Department of Electrical Engineering,
(<http://eesun3.eng.fsu.edu>)*

2525 Pottsdamer Street

Florida A&M University–Florida State University, Tallahassee, Florida 32310-6046

Per Arne Rikvold

*Center for Materials Research and Technology, Department of Physics,
and Supercomputer Computations Research Institute,*

Florida State University, Tallahassee, Florida 32306-3016

*Centre for the Physics of Materials and Department of Physics,
(<http://www.physics.mcgill.ca>)*

McGill University, Montréal, Québec, Canada

(January 15, 2018)

Abstract

An important aspect of real ferromagnetic particles is the demagnetizing field resulting from magnetostatic dipole-dipole interaction, which causes large particles to break up into domains. Sufficiently small particles, however, remain single-domain in equilibrium. This makes such small particles of particular

interest as materials for high-density magnetic recording media. In this paper we use analytic arguments and Monte Carlo simulations to study the effect of the demagnetizing field on the dynamics of magnetization switching in two-dimensional, single-domain, kinetic Ising systems. For systems in the “Stochastic Region,” where magnetization switching is on average effected by the nucleation and growth of fewer than two well-defined critical droplets, the simulation results can be explained by the dynamics of a simple model in which the free energy is a function only of magnetization. In the “Multi-Droplet Region,” a generalization of Avrami’s Law involving a magnetization-dependent effective magnetic field gives good agreement with our simulations.

FSU-SCRI-95-114

PACS Number(s): 75.60.-d, 75.40.Mg, 05.50.+q, 75.10.Hk

Typeset using REVTeX

I. INTRODUCTION

The ability of single-domain ferromagnets to preserve an accurate record of past magnetic fields has several important applications. Fine grains in lava flows preserve a record of the direction of the geomagnetic field at the time they cooled, giving valuable insight into continental drift and the dynamics of the earth’s core.¹ Of more direct technological importance is the potential application of single-domain ferromagnets to magnetic recording media, such as magnetic tapes and disks.

During the magnetic recording process, different regions of the medium are briefly exposed to strong magnetic fields, so that each grain is magnetized in the desired direction.² Since each grain can in principle store one bit of data, a greater storage density could ideally be achieved by a medium containing many small grains than by one containing a few large grains. However, in order to serve as reliable storage devices, the grains must be capable of retaining their magnetizations for long periods of time in weaker, arbitrarily oriented ambient magnetic fields — *i.e.*, they must have a high coercivity and a large remanence. Since experiments show the existence of a particle size at which the coercivity is maximum (see, *e.g.*, Ref. 3), there is a tradeoff between high storage capacity and long-term data integrity which must give rise to an optimum choice of grain size for any given material. During both recording and storage, the relationships between the magnetic field, the size of the grain, and the lifetime of the magnetization opposed to the applied magnetic field are therefore of great technological interest.

Fine ferromagnetic grains have been studied for many years, but until recently such particles could be studied experimentally only in powders (see, *e.g.*, Ref. 3). This made it difficult to differentiate the statistical properties of single-grain switching from effects resulting from distributions in particle sizes, compositions, and local environments, or from interactions between grains. Techniques such as magnetic force microscopy (MFM) (see, *e.g.*, Refs. 4–8) and Lorentz microscopy (see, *e.g.*, Ref. 9) now provide means for overcoming the difficulties in resolving the magnetic properties of individual single-domain particles.

The standard theory of magnetization reversal in single-domain ferromagnets is due to Néel¹⁰ and Brown.¹¹ In order to avoid an energy barrier due to exchange interactions between atomic moments with unlike orientations, Néel-Brown theory assumes uniform rotation of all the atomic moments in the system. The remaining barrier is caused by magnetic anisotropy,¹² which may be either intrinsic or shape-induced. Anisotropy makes it energetically favorable for each atomic moment to be aligned along one or more “easy” axes. Buckling, fanning, and curling are, like uniform rotation, theoretical relaxation processes with few degrees of freedom and global dynamics.^{2,13}

However, for highly anisotropic materials there exists an alternative mode of relaxation with a typically much shorter lifetime. Small regions of the phase in which the magnetization is parallel to the applied magnetic field (the “stable” phase) are continually created and destroyed by thermal fluctuations within the phase in which the magnetization is antiparallel to the field (the “metastable” phase). As long as such a region (henceforth referred to as a “droplet”) is sufficiently small, the short-ranged exchange interaction with the surrounding metastable phase imposes a net free-energy penalty, and the droplet will, with high probability, shrink and vanish. Should the droplet become larger than a critical size, however, this penalty will be less than the benefit obtained from orienting parallel to the magnetic field,

and the droplet will with a high probability grow further, eventually consuming the grain. The nature of the metastable decay thus depends on the relative sizes of the grain, the critical droplet, the average distance between droplets, and the lattice constant, as discussed in detail, *e.g.*, in Refs. 14–17. For systems in which short-range interactions dominate, Fig. 1 sketches the four regions of the space of magnetic fields and particle sizes distinguished by different behaviors during metastable decay. For a more complete, recent review of droplet theory, see Ref. 17.

It is important to understand the difference between a droplet and a domain.¹⁸ Although they are both spatially contiguous regions of uniform magnetization, a domain is an equilibrium feature whereas *a droplet is a strictly non-equilibrium entity*. The domain structure of two-dimensional dipole systems has been extensively investigated.^{19–24} The magnetostatic dipole-dipole interaction produces a demagnetizing field, which results in the stabilization of a domain structure in large ferromagnetic particles at equilibrium.

The purpose of the present paper is to study the effects of long-range dipole-dipole interactions on the *nonequilibrium* phenomenon of magnetization switching in single-domain ferromagnetic particles. Towards this end we employ a simplified model in which particles in equilibrium can have only one or two domains, and we emphasize the single-domain case.

Detailed descriptions of both the static and dynamic properties of fine ferromagnetic grains have typically been formulated from micromagnetic studies.²⁵ This method involves coarse-graining the physical lattice onto a computational lattice and then solving the partial differential equations for the evolution of magnetic structures on the computational lattice. Although micromagnetics provides a good treatment for the anisotropy and demagnetizing fields, it treats thermal effects rather crudely, usually just by making the domain-wall energy temperature-dependent. A somewhat better approximation for thermal fluctuations within the underlying differential equations is to include small fluctuations using a Langevin noise term.²⁶ A better treatment for thermal and time-dependent effects is therefore Monte Carlo simulation (see, *e.g.*, Refs. 27–29). Even when the physical phenomena can be accurately simulated, however, it will be difficult to understand the results without an adequate theoretical basis.

Because of its simplicity, the kinetic nearest-neighbor Ising model has been extensively studied as a prototype for metastable dynamics (see Ref. 17 and references cited therein). In particular, square- and cubic-lattice Ising systems with periodic boundary conditions have been used to study grain-size effects in ferroelectric switching.^{30,31} A related one-dimensional model has been used to study magnetization reversal in elongated ferromagnetic particles.³² In a recent article,³³ we applied statistical-mechanical droplet theory and Monte Carlo simulations of two-dimensional Ising systems to obtain a qualitative approximation for the dynamical behavior of real single-domain particles magnetized opposite to an applied field. In so doing, we made several simplifying approximations, one of which was the absence of a demagnetizing field. In this article we consider the effect of a small demagnetizing field on Ising systems, and compare our analytic calculations with simulations of two-dimensional Ising systems. Specifically, for systems in the Stochastic region (discussed in Sec. III), the demagnetizing fields we consider must be sufficiently small that the system consists of a single domain in equilibrium, whereas in the Multi-Droplet region (discussed in Sec. IV) it is sufficient to have for demagnetizing field to be much smaller than the applied field. Some preliminary results were presented in Ref. 34.

The organization of this paper is as follows. In Sec. II we define the model and numerical methods employed in this paper. In Sec. III we discuss the Stochastic region in terms of an approximate free-energy functional and give some numerical results. In Sec. IV we generalize Avrami's Law,^{35–37} which describes magnetization switching in the Multi-Droplet region, to include the effects of the demagnetizing field, and we compare the analytical results to numerical simulations. Section V contains conclusions and discussions.

II. MODEL AND NUMERICAL METHODS

The standard Ising model is defined by the Hamiltonian

$$\mathcal{H}_0 = -J \sum_{\langle i,j \rangle} s_i s_j - H L^d m, \quad (1)$$

where $s_i = \pm 1$ is the z -component of the magnetization of the atom (spin) at site i , $J > 0$ is the ferromagnetic exchange interaction, and H is the applied magnetic field times the single-spin magnetic moment. The sum $\sum_{\langle i,j \rangle}$ runs over all nearest-neighbor pairs on a square (generally d -dimensional hypercubic) lattice of side L . In this work we do not study the effects of grain boundaries, so periodic boundary conditions are imposed. The dimensionless system magnetization is given by

$$m = L^{-d} \sum_i s_i, \quad (2)$$

where the sum is over all L^d sites. The lattice constant is set to unity.

Addition of dipole-dipole interactions gives a total Hamiltonian (SI units)

$$\mathcal{H}_D = \mathcal{H}_0 + \frac{\mu_0 M^2}{4\pi} \sum_{i \neq j} \frac{s_i s_j}{|\mathbf{r}_{ij}|^3} \left[1 - 3 \left(\frac{\mathbf{r}_{ij}}{|\mathbf{r}_{ij}|} \cdot \hat{\mathbf{z}} \right)^2 \right], \quad (3)$$

where M is the saturation magnetic dipole moment density and \mathbf{r}_{ij} is the vector from site i to site j . Unfortunately, however, the last sum in Eq. (3) slows down Monte Carlo simulations significantly, which is problematic if a large number of realizations are desired for good statistics, as is the case in nonequilibrium studies. The last sum also would make a perturbative expansion in the demagnetizing field (adjustable by changing M or the sample shape) difficult. We therefore instead use the simpler Hamiltonian

$$\mathcal{H}_D = \mathcal{H}_0 + L^d D m^2, \quad (4)$$

where D is a function of the crystal symmetry, the shape of the system, and M . Equations (3) and (4) are equivalent for general ellipsoids *uniformly* magnetized along a principal axis. For the special case of a perpendicularly magnetized plane with square-lattice symmetry, $D = \frac{2}{3} \mu_0 M^2$. For non-uniformly magnetized systems, Eq. (4) amounts to a mean-field treatment of the effects of the dipole-dipole interactions.

For systems with periodic boundary conditions, the exchange and dipole terms of Eq. (4) are equal when the system size is given by¹⁹

$$L_D \approx \frac{2\sigma_\infty(T)}{D [m_{\text{sp}}(T)]^2}, \quad (5)$$

where $\sigma_\infty(T)$ is the surface tension along a primitive lattice vector in the limit $L \rightarrow \infty$ and $m_{\text{sp}}(T)$ is the spontaneous magnetization. For the two-dimensional Ising model, $\sigma_\infty(T)$ ³⁸ and $m_{\text{sp}}(T)$ ³⁹ are known exactly. The length scale on which we would expect a transition from a single-domain to a multi-domain equilibrium structure is approximately L_D .

The selection of the Ising model is equivalent to requiring a very large (infinite, in fact) anisotropy constant. Although magnetic materials used in magnetic recording media require comparatively large anisotropy constants,² the microscopic anisotropy tends to be much smaller than the exchange energy. However, the role of the anisotropy is enhanced by coarse-graining. Simplicity is our main reason for choosing the two-dimensional Ising model with periodic boundary conditions, particularly since many equilibrium properties of the two-dimensional Ising model in zero field are known exactly^{38,39} and since the kinetics of metastable decay has been extensively studied for this model.¹⁷ As a result, our model systems more closely resemble ultrathin magnetic films with perpendicular magnetization than magnetic grains. A more realistic simulation of three-dimensional grains is planned for later study, but we emphasize that we expect that droplet theory applies to almost any spin model with high anisotropy. Accordingly, equations are written in forms appropriate for arbitrary dimensionality d , even though simulations are only carried out for $d=2$.

The relaxation kinetics is simulated by the single-spin-flip Metropolis dynamic with updates at randomly chosen sites. A rigorous derivation from microscopic quantum Hamiltonians of the stochastic Glauber dynamic used in Monte Carlo simulations of Ising models has been established in the thermodynamic limit;⁴⁰ both the Glauber and Metropolis algorithms are spatially local dynamics with non-conserved order parameter (the dynamic universality class of Model A in the classification scheme of Hohenberg and Halperin⁴¹) and are therefore expected to differ only in non-universal features. The Metropolis dynamic is realized by the original Metropolis algorithm⁴² and the n -fold way algorithm.⁴³ (For a discussion on the equivalence of the dynamics of these algorithms, see Ref. 44.) The acceptance probability in the Metropolis algorithm for a proposed flip of the spin at site α from s_α to $-s_\alpha$ is defined as $W(s_\alpha \rightarrow -s_\alpha) = \min[1, \exp(-\beta\Delta E_\alpha)]$, where ΔE_α is the energy change due to the flip and $\beta^{-1} \equiv k_B T$ is the temperature in units of energy. The n -fold way algorithm is similar, but involves the tabulation of energy classes. First an energy class is chosen randomly with the appropriately weighted probability. A single site is then chosen from within that class with uniform probability and flipped with probability one. The number of Metropolis algorithm steps which would be required to achieve this change is chosen from a geometric probability distribution,⁴⁴ and the time, measured in Monte Carlo steps per spin (MCSS), is incremented accordingly. The n -fold way algorithm is more efficient than the Metropolis algorithm at low temperatures, where the Metropolis algorithm requires many attempts before a change is made.

Because we are using single-spin-flip dynamics, the magnetization can only change by a small amount from one time step to the next. The dynamical effects of the demagnetizing field thus depend only on the *change* in the magnetic part of \mathcal{H}_D between adjacent values of the magnetization. In this way it is possible to define an *effective* magnetic field

$$H_{\text{eff}}(H, D, m) \equiv \frac{\partial}{\partial m} (Hm - Dm^2)$$

$$= H - 2Dm . \quad (6)$$

The effective magnetic field is thus site-independent. This fact makes analytic considerations significantly easier and is our principal reason for using Eq. (4) rather than Eq. (3) as the Hamiltonian.

We study the relaxation of the dimensionless system magnetization starting from an initial state magnetized opposite to the applied field [$m(t=0) = +1, H < 0$]. This approach has often been used in previous studies, *e.g.* in Refs. 16,45. For the temperatures employed in this study, the equilibrium spontaneous magnetizations in zero field are close to unity, with $0.95 < m_{\text{sp}} < 1$. Since the applied field is negative (and generally small), the stable magnetization is approximately $m_{\text{st}} \approx -m_{\text{sp}}$ and the metastable magnetization is $m_{\text{ms}} \approx +m_{\text{sp}}$. We use as an operational definition of the lifetime τ of the metastable phase the mean first-passage time to a cutoff magnetization $m=0$:

$$\tau \equiv \langle t(m=0) \rangle . \quad (7)$$

It has been observed¹⁶ that the qualitative results discussed below are not sensitive to the cutoff magnetization as long as it is sufficiently less than m_{sp} . Our choice of $m=0$ as the cutoff facilitates comparison with MFM experiments, which are only capable of measuring the sign of the particle magnetization.

In this paper a numerical subscript indicates the coefficient in a Taylor expansion in D . For example, a quantity X may be expanded $X = X_0 + X_1D + X_2D^2 + \dots$. There are three exceptions to this rule: (1) The subscripts in Eq. (24) refer to an iterative process for evaluating a continued fraction. (2) The subscripts on $\Xi_0(T)$ and $\Xi_1(T)$ [Eq. (26)] indicate an expansion in H^2 and are kept for continuity with Ref. 33. (3) Dummy variables in the Appendix [*e.g.*, Eq. (A2)] may have numerical indices as a matter of convenience.

III. THE STOCHASTIC REGION

It has been shown⁴⁶⁻⁴⁸ that the dynamics of metastable decay in the standard two-dimensional Ising model for sufficiently weak applied field can be semiquantitatively described by a mean-field-like dynamic in which the free energy is a function only of the system magnetization. Under these circumstances switching is abrupt, with a negligible amount of time being spent in configurations with magnetizations significantly different from m_{ms} or m_{st} . Switching is also a Poisson process, with the lifetime of a metastable phase given by the typical Arrhenius form

$$\tau \propto \exp(\beta\Delta F) , \quad (8)$$

where ΔF is the free-energy barrier that must be crossed in the decay process, or by a simple generalization of Eq. (8) if more than one equivalent decay path is present [see Eq. (25)]. This phenomenon, in which the entire system behaves as though it were a single magnetic moment, is known as superparamagnetism.^{12,49} The standard deviation of the switching time for an individual grain is approximately equal to the mean switching time, τ . Because of the random nature of switching in this region, it has been called^{15,16} the ‘‘Stochastic’’ region. The Stochastic region is the union of the ‘‘Coexistence’’ region and the ‘‘Single-Droplet’’ region (discussed below).

In the spirit of Refs. 46–48 we construct an *approximate* restricted free-energy function $F(m)$ for the entire system and use Eq. (8) to illustrate the H - and D -dependence of the lifetime:

$$F(m) = L^d D m^2 + \min\{F_{u,+}(m), F_{u,-}(m), F_{d,+}(m), F_{d,-}(m), F_{sl}(m)\} - F_{sl}(m=0), \quad (9)$$

where $F_{sl}(m)$ is the free energy of a system composed of two “slabs” with magnetizations near $\pm m_{sp}$ [Fig. 2(a) illustrates a “slab” configuration], $F_{d,\pm}(m)$ is the free energy of a system with a single droplet with magnetization near $\mp m_{sp}$ in a background with magnetization near $\pm m_{sp}$ [Fig. 2(b) illustrates a “single droplet” configuration], and $F_{u,\pm}(m)$ is the free energy of a system in a “uniform” phase near $m = \pm m_{sp}$. Figure 3 illustrates $\beta F(m)$ for $L \ll L_D$, $L = L_D$, and $L \gg L_D$.

We approximate the free energy of a system in a “uniform” phase by

$$F_{u,\pm}(m) \equiv -L^d H m + L^d \frac{1}{2} \chi^{-1} (m \mp m_{sp})^2, \quad (10)$$

where χ is the equilibrium susceptibility per spin. Since an exact solution for the two-dimensional Ising model in a magnetic field has not yet been found, we use instead an estimate from a series expansion,⁵⁰ so that for $T = 0.8T_c$, $\chi \approx 0.05J^{-1}$.

Minimizing $F_{u,-}(m) + L^d D m^2$ yields the stable magnetization m_{st} , which is the location of the global minimum of $F(m)$ for $L < L_D$:

$$m_{st} \approx \frac{-m_{sp} + H\chi}{1 + 2D\chi} \quad (11a)$$

(remember, $H < 0$). Likewise, for $L \ll L_D$ the next-lowest minimum of $F(m)$ is obtained by minimizing $F_{u,+}(m) + L^d D m^2$:

$$m_{ms} \approx \frac{m_{sp} + H\chi}{1 + 2D\chi}. \quad (11b)$$

Equation (11a) is valid for a wider range of H than is Eq. (11b). We shall refer to m_{ms} as the “metastable magnetization” and its basin of attraction as the “metastable phase”, since for systems of interest ($L < L_D$) the length of time required for a system initially prepared in the metastable phase to escape to the stable phase is much longer than any other timescale. Note, however, that other, shorter-lived metastable phases may exist (discussed below).

In cases where the magnetization differs significantly from m_{sp} ($-m_{sp}$), a lower free energy can often be obtained by segregating the system into a single localized “droplet” with magnetization near m_{st} (m_{ms}) in a background with magnetization near m_{ms} (m_{st}).⁵¹ Specifically, the droplet free energy is approximated by

$$F_{d,+}(m) \equiv \Omega \left[d\sigma_{\infty} R_+^{d-1} + (m_{ms} - m_{st}) H R_+^d \right] - L^d H m_{ms} \quad (12a)$$

and

$$F_{d,-}(m) \equiv \Omega \left[d\sigma_{\infty} R_-^{d-1} - (m_{ms} - m_{st}) H R_-^d \right] - L^d H m_{st} \quad (12b)$$

subject to $m_{ms} > m > m_{st}$. Here

$$R_+ = \Omega^{-1/d} L \left(\frac{m_{\text{ms}} - m}{m_{\text{ms}} - m_{\text{st}}} \right)^{1/d} \quad (13a)$$

is the radius of a droplet of “down” (stable) spins in an “up” (metastable) background,

$$R_- = \Omega^{-1/d} L \left(\frac{m - m_{\text{st}}}{m_{\text{ms}} - m_{\text{st}}} \right)^{1/d} \quad (13b)$$

is the radius of a droplet of “up” (metastable) spins in a “down” (stable) background. For $T \not\approx 0$, the droplet shape can be found from a Wulff construction. The quantity Ω , which gives the volume of the droplet via $V = \Omega R^d$, can be found to arbitrary precision for the two-dimensional Ising model by numerically integrating over the exactly known surface tension.^{52,53}

Lastly, near $m=0$ the circumference of the droplet becomes larger than twice the cross-section of the system, and the lowest free energy is obtained by segregating the system into two slab-like configurations.⁵⁴ The corresponding slab free energy is approximated by

$$F_{\text{sl}}(m) \equiv 2L^{d-1}\sigma_\infty - L^d H m. \quad (14)$$

Comparison with Eq. (12) shows that $F(m) = F_{\text{sl}}(m)$ for $m_{\text{ds},+} \geq m \geq m_{\text{ds},-}$, where^{48,54}

$$m_{\text{ds},+} = m_{\text{ms}} - (m_{\text{ms}} - m_{\text{st}})\Omega^{-1/(d-1)} \left(\frac{2}{d} \right)^{d/(d-1)} > 0 \quad (15a)$$

and

$$m_{\text{ds},-} = m_{\text{st}} + (m_{\text{ms}} - m_{\text{st}})\Omega^{-1/(d-1)} \left(\frac{2}{d} \right)^{d/(d-1)} < 0. \quad (15b)$$

Note that for $D > H/(2m_{\text{ds},-})$, a local minimum of $F(m)$ occurs for a slab configuration at $m = H/(2D)$. For $L < L_D$ it is a metastable phase, but for $L \geq L_D$ and $D > H/m_{\text{st}}$ it is the global minimum of $F(m)$ and hence the true stable phase (see Fig. 3). Other interesting features can be obtained by solving $(d/dm) [L^d D m^2 + F_{\text{d},\pm}(m)] = 0$, which can in general be done only numerically. This reveals that near $L = L_D$ short-lived metastable phases can exist for $m > m_{\text{ds},+}$ or $m < m_{\text{ds},-}$.

For $L < L_D$, the system enjoys true coexistence at zero applied field between two degenerate equilibrium phases with magnetizations m_{ms} and m_{st} . This leads to the identification^{15,16} of a “Coexistence” (CE) region within which $F(m_{\text{ms}}) \approx F(m_{\text{st}})$. Within the CE region, the free energy barrier for tunnelling from the metastable phase to the stable phase is approximately the same as the free energy barrier for tunnelling from the stable phase to the metastable phase, so the decay process is both stochastic and reversible. Specifically, for $L \ll L_D$, the lifetime of the metastable phase is given by Eq. (8) with $\Delta F = F(m_{\text{ds},+}) - F(m_{\text{ms}})$, so that^{55–57}

$$\tau(L, H, T) \approx A(T) \exp \left\{ \beta \left[2\sigma_\infty(T) L^{d-1} - L^d |H| (m_{\text{ms}} - m_{\text{ds},+}) - L^d D (m_{\text{ms}}^2 - m_{\text{ds},+}^2) \right] \right\}, \quad (16)$$

where $A(T)$ is a non-universal prefactor.

For $L \approx L_D$, the maximum of $F(m)$ occurs not at $m_{\text{ds},+}$ but at a larger magnetization corresponding to a single critical droplet. The size of this droplet, however, is strongly dependent on the system size L . This part of the Coexistence region is further complicated by the increasing importance of the metastable phase at $m = H/(2D)$ and the aforementioned possibility of metastable phases near $m = m_{\text{ds},\pm}$.

For $H \gg D$ the maximum of $F(m)$ may correspond to a critical droplet the size of which is nearly independent of system size since it is determined by the *applied* field rather than the *demagnetizing* field. The applied field at which the CE region crosses over into this ‘‘Single Droplet’’ (SD) region^{15,16} is called^{15,16} the ‘‘Thermodynamic Spinodal’’ (H_{ThSp}). A useful estimate for this crossover is $(d/dm) [L^d D m^2 + F_{\text{d},+}(m)]|_{m_{\text{ds},+}} = 0$, yielding⁴⁸

$$|H_{\text{ThSp}}| \approx L^{-1} \Omega^{1/(d-1)} \frac{(d-1)\sigma_\infty}{m_{\text{ms}} - m_{\text{st}}} \left(\frac{d}{2}\right)^{1/(d-1)} - 2Dm_{\text{ds},+}. \quad (17)$$

A slightly different estimate was used in Ref. 17 and Ref. 33, but the two estimates are approximately equal.

In the SD region the first critical droplet to nucleate almost always grows to fill the system before any other droplet nucleates. The average time required to nucleate the first droplet can be estimated from Eq. (8), where the free-energy barrier is determined from Eq. (10) and Eq. (12a). Since the SD region is also the region of weak H and D , we can obtain a good approximation by neglecting terms of $O(H_{\text{eff}}\chi)$. Then the magnetization in the metastable background is $m_{\text{ms}} = m_{\text{sp}}$, and inside the droplet it is $m_{\text{st}} = -m_{\text{sp}}$. In terms of the droplet radius R , the difference between the free energy of a system containing one droplet and that of a uniform metastable system can then be written as

$$\Delta F(R) = d\Omega\sigma_\infty(T)R^{d-1} - 2m_{\text{sp}}(|H| + 2Dm_{\text{sp}})\Omega R^d + 4Dm_{\text{sp}}^2 L^{-d}\Omega^2 R^{2d}. \quad (18)$$

Differentiating with respect to R , we find the implicit equation satisfied by the critical droplet radius:

$$R_c(T, H, D) = \frac{(d-1)\sigma_\infty(T)}{2m_{\text{sp}}|H_{\text{eff},c}(H, D)|}, \quad (19a)$$

where

$$|H_{\text{eff},c}(H, D)| = |H| + 2Dm_{\text{sp}} [1 - 2\Omega (R_c/L)^d] \quad (19b)$$

is the effective field evaluated at the magnetization of a system containing a single, critical droplet. Note that $H_{\text{eff},c}$ depends on $|H|$ and D explicitly, as well as implicitly through R_c . For $D=0$, Eq. (19) reduces to the standard expression for R_c .¹⁷ By inserting R_c into Eq. (18) one finds that the free-energy barrier corresponding to the critical droplet is also simply given by a standard expression,¹⁷ in which $|H|$ has been replaced by $|H_{\text{eff},c}|$:

$$\beta\Delta F_{\text{SD}} = \frac{\Xi_0(T)}{|H_{\text{eff},c}(H, D)|}, \quad (20)$$

where¹⁷

$$\Xi_0(T) \equiv \beta\Omega [\sigma_\infty(T)]^d \left(\frac{d-1}{2m_{\text{sp}}} \right)^{d-1}. \quad (21)$$

Note that $\Xi_0(T)$ is completely defined by quantities that for the two-dimensional Ising model are either known exactly (σ_∞ and m_{sp})^{38,39} or can be obtained by numerical integration of exactly known quantities (Ω).^{52,53}

The above results indicate that in order to obtain the nucleation rate for nonzero D , one only needs to determine $|H_{\text{eff},c}|$. This can easily be done to arbitrary numerical precision via a rapidly convergent, generalized continued-fraction expansion as follows.

Let $x = 2Dm_{\text{sp}}/|H|$ be the reduced demagnetization field and $V(x) = 2\Omega(R_c/L)^d$ be the volume fraction occupied by the critical droplet. Then

$$|H_{\text{eff},c}| = |H| \{1 + x [1 - V(x)]\} \equiv |H| y(x), \quad (22)$$

and $V(x)$ is given by the generalized continued-fraction expansion,

$$V(x) = \frac{V_0}{\left[1 + x \left(1 - \frac{V_0}{\left[1 + x \left(1 - \frac{V_0}{[\dots]^d} \right) \right]^d} \right) \right]^d}, \quad (23)$$

where $V_0 = V(0)$. This expansion can be evaluated to desired precision by the recursion relation,

$$V_n = \frac{V_0}{[1 + x(1 - V_{n-1})]}. \quad (24)$$

(Here the subscript is proportional to the order of a rational-function approximation to the generalized continued fraction, rather than denoting the order of a term in a power series in D , as elsewhere in this paper.)

The lifetime in the SD region can be given in terms of the nucleation rate per unit volume I by¹⁷

$$\tau \approx [L^d I]^{-1}. \quad (25)$$

For $D=0$ and $\chi \approx 0$, I has been shown to be given by¹⁷

$$I(T, H) \approx B(T) |H|^K \exp \left\{ -|H|^{1-d} [\Xi_0(T) + \Xi_1(T) H^2] \right\}, \quad (26)$$

where $B(T)$ is a non-universal prefactor, and K is believed to be 3 for the two-dimensional Ising model and $-1/3$ for the three-dimensional Ising model.¹⁶ (The subscripts on $\Xi_0(T)$ and $\Xi_1(T)$ indicate an expansion in H^2 rather than in D , and are kept for consistency with the notation in Ref. 33.) The quantity $\Xi_0(T)$ is given by Eq. (21), and we determine $\Xi_1(T)$ from a numerical fit to the H -dependence of the lifetime. Note that the lifetime obtained from Eqs. (25) and (26) is quite similar to the Arrhenius form with the free-energy barrier given by Eq. (20). The only differences are the prefactor $|H|^{-K}$ and the term $\Xi_1(T) H^2$ in the

exponential, which are due to surface fluctuations on the droplet and to higher-order terms in a field-theoretical calculation of the free-energy barrier, respectively.¹⁷ We generalize to the $D \neq 0$ case by assuming that the nucleation rate in the SD region is given by Eq. (26) with $|H|$ replaced by $|H_{\text{eff},c}(H, D)|$, as we have already shown in Eq. (20) for the dominant term in the free-energy barrier, ΔF_{SD} . The resulting expression for the relative lifetime for nonzero D is then given by

$$\frac{\tau(x)}{\tau(0)} = y(x)^{-K} \exp \left\{ -\Xi_0 |H|^{1-d} [1 - y(x)^{1-d}] - \Xi_1 |H|^{3-d} [1 - y(x)^{3-d}] \right\}, \quad (27)$$

where $y(x)$ is defined in Eq. (22). This result is shown in Fig. 4, together with MC data, for $d=2$, $T=0.8T_c$, $H=0.2J$, and $L=10$. Except for Ξ_1 , the parameters needed to evaluate $\tau(x)/\tau(0)$ are known exactly or numerically exactly for the two-dimensional Ising model: $V_0=0.2399(1)$ and $\Xi_0=0.5062(1)$. The value of Ξ_1 used in Fig. 4, $\Xi_1 = 9.1(3)J^{-1}$, was obtained in Ref. 33 from the $|H|$ dependence of τ for $D=0$ in the SD region. Thus the good agreement seen in Fig. 4 between the simulation data and the theoretical prediction is not the result of a fit to the data, but is determined entirely from quantities measured with $D=0$.

IV. THE MULTI-DROPLET REGION

For sufficiently strong fields or large systems, decay occurs through many weakly interacting droplets in the manner described by Kolmogorov,³⁵ Johnson and Mehl,³⁶ and Avrami.³⁷ Such decay is “deterministic” in the sense that the standard deviation of the switching time is much less than its mean (see Ref. 33 for details). The crossover between the SD region and the Multi-Droplet (MD) region has been called^{15,16} the “Dynamic Spinodal” (DSp). Since the standard deviation of the lifetime is equal to its mean in the Stochastic region, we estimate this crossover by the field $H_{1/2}$ at which

$$\sqrt{\langle t^2(m=0) \rangle - \tau^2} = \frac{\tau}{2}. \quad (28)$$

For *asymptotically* large L , $H_{\text{DSp}} \sim (1/\ln L)^{1/(d-1)}$,^{16,33} however, prohibitively large system sizes may be required before this scaling form is observed. At a sufficiently high field, nucleation becomes much faster than growth and the droplet picture breaks down. The crossover to this “Strong-Field” region (SF) has been called^{15,16} the “Mean-Field Spinodal” (MFSp). A conservative estimate for this crossover field is obtained by setting $2R_c=1$:

$$|H_{\text{MFSp}}| \approx \frac{(d-1)\sigma_\infty(T)}{m_{\text{sp}}}. \quad (29)$$

Little is understood quantitatively about the SF region.

In this section we generalize Avrami’s Law^{35–37} to systems with nonzero D . Avrami’s Law gives the volume fraction of the metastable phase (or equivalently, the magnetization) for systems in which droplets nucleate with a constant rate (per unit volume) I_0 and grow at constant velocity v_0 without interacting except for overlaps. The generalization we make

below is for a nucleation rate and velocity that depend on the magnetization, and through it on time.

The time-dependent mean system magnetization $m(t)$ is given by

$$m(t) = (m_{\text{ms}} - m_{\text{st}})e^{-\Phi(t)} + m_{\text{st}} . \quad (30)$$

Here

$$\Phi(t) \equiv \int_0^t I(t')V(t', t)dt' \quad (31)$$

is the mean volume fraction of droplets (uncorrected for overlap) and

$$V(t_1, t_2) \equiv \Omega \left[\int_{t_1}^{t_2} v(t)dt \right]^d \quad (32)$$

is the volume occupied by a droplet which nucleates at time t_1 and grows with a time-dependent radial velocity $v(t)$ until time t_2 . Here $v(t)$ is the (nonuniversal) temperature-dependent radial growth velocity of a droplet, which under an Allen-Cahn approximation^{58–61} is proportional to the effective field in the limit of large droplets:

$$v(t) \approx \nu \left| H_{\text{eff}}(H, D, m(t)) \right| . \quad (33)$$

The time-dependent nucleation rate is given by $I(t) \equiv I[T, H_{\text{eff}}(H, D, m(t))]$ from Eq. (26). Note how this differs from the D -dependent nucleation rate in the SD region. In the SD region, the D -dependence of the nucleation rate comes from the change in system magnetization from the nucleation of a single critical droplet. In the MD region, by contrast, we ignore the change in system magnetization due to the nucleation of a *single* droplet (since $L \gg R_c$), and the D -dependence of the nucleation rate comes from the change in system magnetization due to an *ensemble* of droplets.

For $D=0$, Eq. (30) becomes^{35–37}

$$m_0(t) = (m_{\text{ms},0} - m_{\text{st},0})e^{-\Phi_0(t)} + m_{\text{st},0} , \quad (34)$$

where

$$\Phi_0(t) = \ln \left(\frac{m_{\text{ms},0} - m_{\text{st},0}}{|m_{\text{st},0}|} \right) \left(\frac{t}{\tau_0} \right)^{d+1} , \quad (35)$$

so that τ_0 is the first-passage time to $m=0$ [Eq. (7)]. Specifically, τ_0 is given by^{35–37}

$$\tau_0 = \left[\frac{I_0 \Omega v_0^d}{(d+1) \ln z_0} \right]^{-\frac{1}{d+1}} , \quad (36)$$

where

$$z_0 \equiv \frac{m_{\text{ms},0} - m_{\text{st},0}}{|m_{\text{st},0}|} \approx 2 . \quad (37)$$

In Eq. (37) and elsewhere in this section, the estimate for the metastable magnetization given by Eq. (11b) does not suffice. Ramos *et al.* have estimated $m_{\text{ms}}(H)$ by extrapolating

$m(t)$ back to $t=0$ assuming that $m(t)$ is correctly described by Avrami's Law.⁶² (Since the initial condition is $m_0 = 1$ rather than $m_0 = m_{\text{ms}}$, the earliest times must be discarded.) These estimates are shown in Fig. 5. We fit a smooth curve through the data, insisting that $m_{\text{ms}}(0) \equiv m_{\text{sp}}$ and $(d/dH)m_{\text{ms}}|_{H=0} = \chi$. The smooth curve allows us to estimate the change in m_{ms} due to D , but the correct form of $m_{\text{ms}}(H)$ is not known.

For $D=0$, the standard deviation of the time-dependent magnetization has been shown to vanish with increasing system size as $L^{-d/2}$,^{33,63} a feature which is shared by the more general case of $D \geq 0$. In fact, realizations in which the magnetization chances to decay more rapidly than average will experience a weaker effective field [Eq. (6)], and realizations in which the magnetization decays more slowly than average will experience a stronger effective field. These effects combine to cause systems with $D > 0$ to have even smaller standard deviations in their time-dependent magnetizations than corresponding systems with $D=0$.

To first order in D , the effective magnetic field [from Eq. (6)] is given by

$$H_{\text{eff}}(H, D, m(t)) \approx H - 2Dm_0(t) \quad (38)$$

since any D -dependent terms in $m(t)$ will lead to only higher-order corrections. We will expand $\Phi(t)$ to first order in D , so that we can use the known value of $m_0(t)$ instead of the unknown value $m(t)$ on the right-hand side of Eq. (31). In order to perform the expansion correctly, we must expand $I(t)$ and $V(t_1, t_2)$ to first order in D . Specifically, the total volume fraction (uncorrected for overlap) of droplets after a time t is given by

$$\Phi(t) \approx \Phi_0(t) + \Phi_1(t)D \quad (39)$$

where

$$\Phi_1(t) \equiv \Phi_V(t) + \Phi_I(t), \quad (40)$$

$$\Phi_V(t) \equiv \int_0^t I_0 V_1(t', t) dt', \quad (41)$$

and

$$\Phi_I(t) \equiv \int_0^t I_1(t') V_0(t', t) dt'. \quad (42)$$

Straightforward but cumbersome mathematics shows (see the Appendix)

$$\begin{aligned} \Phi_V(t) \approx 2(d)|H|^{-1}|m_{\text{st},0}| & \left\{ -\Phi_0(t) + \frac{z_0}{d} [\Phi_0(t)]^{d/(d+1)} \gamma \left[\frac{1}{d+1}, \Phi_0(t) \right] \right. \\ & \left. + \frac{z_0}{d+1} \sum_{k=0}^{d-1} \binom{d-1}{k} (-1)^{d-k} [\Phi_0(t)]^{k/(d+1)} \mathcal{A} \left[\frac{-(k+1)}{d+1}, \frac{1}{d+1}, \Phi_0(t) \right] \right\} \quad (43) \end{aligned}$$

and

$$\begin{aligned} \Phi_I(t) \approx \lambda(H)|m_{\text{st},0}| & \left(z_0 \sum_{k=0}^d \left\{ \binom{d}{k} (-1)^{d-k} [\Phi_0(t)]^{k/(d+1)} \gamma \left[1 - \frac{k}{d+1}, \Phi_0(t) \right] \right\} \right. \\ & \left. - \Phi_0(t) \right), \quad (44) \end{aligned}$$

where

$$\lambda(H) \equiv 2 \left\{ \frac{K}{|H|} + |H|^{-d} [(d-1)\Xi_0 + (d-3)\Xi_1 H^2] \right\}, \quad (45)$$

comes from differentiating Eq. (26) with respect to H , γ denotes the incomplete gamma function

$$\gamma(a, x) \equiv \int_0^x y^{a-1} e^{-y} dy, \quad (46)$$

and \mathcal{A} is given by

$$\mathcal{A}(a, b, x) \equiv \int_0^x y^a \gamma(b, y) dy. \quad (47)$$

Both γ and \mathcal{A} are easily evaluated by Taylor series.

We can insert $\Phi_V(t)$ and $\Phi_I(t)$ into Eq. (40) to find $\Phi_1(t)$ and then use Eq. (30) to evaluate

$$m_1(t) = (m_{\text{ms},1} - m_{\text{st},1})e^{-\Phi_0(t)} + m_{\text{st},1} - (m_{\text{ms},0} - m_{\text{st},0})e^{-\Phi_0(t)}\Phi_1(t). \quad (48)$$

Finding the second-order terms in D proceeds along parallel lines. Although it is possible to find an analytic expression for $m_2(t)$, this expression is tedious to derive and unenlightening. Furthermore, enough approximations have already been introduced to make the significance of an analytic expression for $m_2(t)$ suspect. Consequently, we estimate $m(t)$ by integrating Eq. (31) numerically with the effective field $H - 2D[m_0(t) + Dm_1(t)]$. The resulting estimate we denote $m_f(t)$, and it should be approximately correct to $O(D^2)$. If necessary, this process can be iterated to find successively better approximations for $m(t)$.

Figure 6 shows the time-dependence of the the magnetization, both as approximated above and as simulated by Monte Carlo. For Ξ_1 we have used $\Xi_1 = 3.0(3)$, as determined in Ref. 33 from the $|H|$ dependence of τ for $D=0$ in the MD region. Note that there is good agreement between the simulation results and the approximation after an initial relaxation into the metastable phase, and that the modification to $m(t)$ resulting from higher-order terms is minor.

In order to calculate the effect of D on the lifetime, we start with $m(\tau) \equiv 0$ and expand both m and τ in D . Collecting terms and discarding all terms of higher order than D^2 , we find

$$0 = \{m_0(\tau_0)\} + \left\{ m_1(\tau_0) + \tau_1 \left. \frac{dm_0}{dt} \right|_{\tau_0} \right\} D + \left\{ m_2(\tau_0) + \tau_1 \left. \frac{dm_1}{dt} \right|_{\tau_0} + \tau_2 \left. \frac{dm_0}{dt} \right|_{\tau_0} + \frac{1}{2} \tau_1^2 \left. \frac{d^2 m_0}{dt^2} \right|_{\tau_0} \right\} D^2. \quad (49)$$

Since the quantities in the braces are independent of D and Eq. (49) is true for all small D , by necessity $m_0(\tau_0) = 0$,

$$\tau_1 = -m_1(\tau_0) \left[\left. \frac{dm_0}{dt} \right|_{\tau_0} \right]^{-1}, \quad (50)$$

and

$$\tau_2 = - \left[m_2(\tau_0) + \tau_1 \left. \frac{dm_1}{dt} \right|_{\tau_0} + \frac{1}{2} \tau_1^2 \left. \frac{d^2 m_0}{dt^2} \right|_{\tau_0} \right] \left[\left. \frac{dm_0}{dt} \right|_{\tau_0} \right]^{-1}. \quad (51)$$

Equation (50) is readily evaluated because $\Phi_0(t)$ is a simple function. It is likewise simple to calculate $(d^2 m_0/dt^2)|_{\tau_0}$ for use in Eq. (51). We have not actually solved for $m_2(t)$, but for small D we can use

$$m_2(t) \approx D^{-2} \left\{ m_f(t) - [m_0(t) + Dm_1(t)] \right\}. \quad (52)$$

Finally, $(dm_1/dt)|_{\tau_0}$ can be evaluated by differentiating Eq. (43) and Eq. (44) with respect to t :

$$\begin{aligned} \left. \frac{d}{dt} \Phi_V(t) \right|_{t=\tau_0} &\approx 2(d) |H|^{-1} |m_{\text{st},0}| \frac{(d+1) \ln z_0}{\tau_0} \\ &\times \left\{ -1 + \frac{1}{d} \frac{z_0}{d+1} (\ln z_0)^{-1/(d+1)} \gamma \left(\frac{1}{d+1}, \ln z_0 \right) \right. \\ &+ \frac{z_0}{(d+1)^2} \sum_{k=0}^{d-1} \binom{d-1}{k} (-1)^{d-k} k (\ln z_0)^{(k-d-1)/(d+1)} \\ &\left. \mathcal{A} \left(\frac{-(k+1)}{d+1}, \frac{1}{d+1}, \ln z_0 \right) \right\} \end{aligned} \quad (53)$$

and

$$\begin{aligned} \left. \frac{d}{dt} \Phi_I(t) \right|_{t=\tau_0} &\approx \lambda(H) |m_{\text{st},0}| \frac{(d+1) \ln z_0}{\tau_0} \left(-1 + \frac{z_0}{d+1} \sum_{k=0}^d \left\{ \binom{d}{k} (-1)^{d-k} k \right. \right. \\ &\left. \left. \times (\ln z_0)^{(k-d-1)/(d+1)} \gamma \left(1 - \frac{k}{d+1}, \ln z_0 \right) \right\} \right). \end{aligned} \quad (54)$$

This yields $(d\Phi_1/dt)|_{\tau_0}$ from Eq. (40). Once this is known, differentiating Eq. (48) is trivial, and τ_2 can easily be evaluated.

Figure 7 shows τ vs. D for two different values of H . The agreement between the theoretical curves and the Monte Carlo data is again excellent. Once again, the theoretical curves are not fits to the simulation data, but use only parameters determined for $D=0$, namely, $m_{\text{ms}}(H)^{62}$ and $\Xi_1(T)$.³³

V. DISCUSSION

Due to the importance of magnetic recording technologies in modern society, magnetic relaxation has been a subject of study for many years. However, even the equilibrium thermodynamics of magnetic materials is very difficult to predict from first principles and generally has to be approximated from simpler models (see, *e.g.*, Ref. 64). As a result, the most popular method for theoretical investigation of magnetization reversal involves setting up and solving differential equations on a lattice obtained by course-graining over

the microscopic crystal lattice. This method, known as micromagnetics,²⁵ often gives very good results, particularly for equilibrium studies or for multi-domain particles. However, micromagnetic calculations take thermal effects into account only crudely.

An alternative method is to treat the statistical mechanics carefully, making simplifications to the model until it can be well understood. This is the approach we take. In Ref. 33 we showed that both the switching field and the probability that the magnetization is greater than zero, calculated from Monte Carlo simulations of the two-dimensional Ising model, are qualitatively similar to the same quantities measured in isolated, well characterized single-domain ferromagnets by techniques such as MFM. Since statistical-mechanical droplet theory successfully explains the Ising model simulations, it is plausible that droplet theory could also be applied to the experimental particles.

In this article we consider the effect of the magnetic dipole-dipole interaction, which was neglected in Ref. 33. By treating the dipole-dipole interaction in a mean-field approximation, we are able to calculate droplet-theory predictions for the lifetime for systems in which magnetic decay occurs by means of a single droplet (Fig. 4). We also obtain both the time-dependent magnetization (Fig. 6) and the lifetime (Fig. 7) for systems in which magnetic decay occurs through the action of many droplets. In all of these figures, all parameters were determined by measurements at $D=0$, so the excellent agreements are not the result of curve fitting.

It should be pointed out that the droplet-theory predictions made in both the Single-Droplet and Multi-Droplet regions are large-droplet approximations. Since a critical droplet in the two-dimensional Ising model at $T=0.8T_c$ and $|H|=0.3J$ consists of approximately six overturned spins, it is quite remarkable that these expressions give the good approximations they do.

In Ref. 27, Kirby *et al.* use the two-dimensional Ising model with mean-field dipole-dipole interactions to simulate Dy/Fe ultrathin films which they have observed experimentally, obtaining good agreement. The analytic results from Sec. IV are directly applicable to such films, although different values of T , H , and D must be chosen to make the comparison. However, care should be used in applying the results. Specifically, if $|Dm_{sp}/H|$ is not small, more numerical iterations of the type described in Sec. IV will be necessary, and if $|H_{\text{eff}}| \gtrsim |H_{\text{MFSp}}|$ [Eq. (29)], droplet theory may not be applicable.

It is interesting to note that the mean-field demagnetizing field we have used does not change the qualitative behavior of the switching field as a function of system size from that which was studied in Ref. 33 and sketched in Fig. 1. Although the values of the switching field are reduced, a peak in the switching field still occurs near the thermodynamic spinodal, as can be seen by comparing Eq. (16) and Eq. (25). Furthermore, the switching field remains roughly independent of L in the MD region. What is noticeably absent is any feature at $L = L_D$; the switching field shows features due to transitions in the dynamics, but not transitions in the statics.

Even with the addition of the demagnetizing field, the Ising model remains too crude a model for magnetism to describe quantitatively real magnetic materials, except perhaps for some ultrathin films as noted above. Heterogenous nucleation at boundaries, quenched disorder, and more realistic anisotropies are therefore planned as the subject of future studies.

ACKNOWLEDGMENTS

The authors wish to thank B. M. Gorman and R. A. Ramos for useful discussions and for comments on the manuscript. We also wish to thank S. W. Sides for Fig. 2(b), and R. A. Ramos for providing the data on which Fig. 5 is based prior to publication. During the final stages of this work, H. L. R. and P. A. R. enjoyed the hospitality and support of the Risø National Laboratory and McGill University, respectively. This research was supported in part by the Florida State University Center for Materials Research and Technology, by the FSU Supercomputer Computations Research Institute, which is partially funded by the U. S. Department of Energy through Contract No. DE-FC05-85ER25000, and by the National Science Foundation through Grants No. DMR-9315969 and DMR-9520325. Computing resources at the National Energy Research Supercomputer Center were made available by the U. S. Department of Energy.

APPENDIX: AVRAMI'S LAW FOR $D \geq 0$

In this Appendix we give some of the steps that have been omitted for clarity in Sec. IV. Beginning with the Allen-Cahn approximation^{58–61} for the radial growth velocity [Eq. (33)] and with the effective magnetic field to $O(D)$ [Eq. (6)], we find

$$v(t) \approx v_0 \left[1 + \frac{2D}{|H|} m_0(t) \right]. \quad (\text{A1})$$

Substituting Eq. (A1) into Eq. (32), we find

$$\begin{aligned} V(t_1, t_2) &\approx \Omega v_0^d \left\{ \int_{t_1}^{t_2} \left[1 + \frac{2D}{|H|} m_0(t) \right] dt \right\}^d \\ &\approx \Omega v_0^d \left[(t_2 - t_1)^d + \binom{d}{1} \frac{2D}{|H|} (t_2 - t_1)^{d-1} \int_{t_1}^{t_2} m_0(t) dt \right]. \end{aligned} \quad (\text{A2})$$

This enables us to make the identifications

$$V_0(t_1, t_2) = \Omega v_0^d (t_2 - t_1)^d \quad (\text{A3})$$

and

$$V_1(t_1, t_2) = 2\Omega v_0^d \binom{d}{1} |H|^{-1} (t_2 - t_1)^{d-1} \int_{t_1}^{t_2} m_0(t) dt. \quad (\text{A4})$$

A Taylor expansion of the nucleation rate [Eq. (26)]

$$\begin{aligned} I(t) &\approx I_0 + \left. \frac{dI}{dD} \right|_0 D = I_0 + \left. \frac{dI}{d|H_{\text{eff}}|} \right|_0 \left. \frac{d|H_{\text{eff}}|}{dD} \right|_0 D \\ &= I_0 + \left. \frac{dI}{d|H_{\text{eff}}|} \right|_0 [2m_0(t)] D \end{aligned} \quad (\text{A5})$$

yields

$$I_1(t) = \lambda(H)I_0m_0(t), \quad (\text{A6})$$

where $\lambda(H)$ is given by Eq. (45).

The evaluation of $\Phi_I(t)$ and $\Phi_V(t)$ can be followed more easily if the reader keeps in mind three basic “tricks”: we apply of the binomial theorem,

$$(t - t')^n = \sum_{k=0}^n t^k (-t')^{n-k} \binom{n}{k}, \quad (\text{A7})$$

we use Eq. (36) to simplify expressions, and we make changes of variables of the form $x = \Phi_0(t')$. These lead to expressions such as

$$(d+1) \left(\frac{\ln z_0}{\tau_0^{d+1}} \right)^{(n+1)/(d+1)} t^k (t')^{n-k} dt' = [\Phi_0(t)]^{k/(d+1)} x^{(n-k-d)/(d+1)} dx. \quad (\text{A8})$$

Using Eq. (34) in Eq. (A4)

$$\begin{aligned} V_1(t_1, t_2) &\approx 2\Omega v_0^d \binom{d}{1} |H|^{-1} (t_2 - t_1)^{d-1} |m_{\text{st},0}| \\ &\quad \times \int_{t_1}^{t_2} \left\{ z_0 \exp \left[-\ln(z_0) \left(\frac{t}{\tau_0} \right)^{d+1} \right] - 1 \right\} dt \\ &= 2 \binom{d}{1} |H|^{-1} |m_{\text{st},0}| \left[-V_0(t_1, t_2) + \Omega v_0^d \frac{z_0}{d+1} (\ln z_0)^{-1/(d+1)} (t_2 - t_1)^{d-1} \tau_0 \right. \\ &\quad \left. \times \int_{\Phi_0(t_1)}^{\Phi_0(t_2)} e^{-x} x^{\frac{1}{d+1}-1} dx \right] \\ &= 2 \binom{d}{1} |H|^{-1} |m_{\text{st},0}| \left(-V_0(t_1, t_2) + \Omega v_0^d \frac{z_0}{d+1} (\ln z_0)^{-1/(d+1)} (t_2 - t_1)^{d-1} \tau_0 \right. \\ &\quad \left. \times \left\{ \gamma \left[\frac{1}{d+1}, \Phi_0(t_2) \right] - \gamma \left[\frac{1}{d+1}, \Phi_0(t_1) \right] \right\} \right). \quad (\text{A9}) \end{aligned}$$

Using Eq. (A9) in Eq. (41),

$$\begin{aligned} \Phi_V(t) &\approx 2 \binom{d}{1} |H|^{-1} |m_{\text{st},0}| \left(-\Phi_0(t) + I_0 \Omega v_0^d \frac{z_0}{d+1} (\ln z_0)^{-1/(d+1)} \tau_0 \right. \\ &\quad \left. \times \left\{ \frac{t^d}{d} \gamma \left[\frac{1}{d+1}, \Phi_0(t) \right] - \int_0^t (t-t')^{d-1} \gamma \left[\frac{1}{d+1}, \Phi_0(t') \right] dt' \right\} \right) \\ &= 2 \binom{d}{1} |H|^{-1} |m_{\text{st},0}| \left(-\Phi_0(t) + z_0 (\ln z_0)^{d/(d+1)} \tau_0^{-d} \right. \\ &\quad \left. \times \left\{ \frac{t^d}{d} \gamma \left[\frac{1}{d+1}, \Phi_0(t) \right] - \int_0^t \sum_{k=0}^{d-1} \binom{d-1}{k} t^k (-t')^{d-1-k} \gamma \left[\frac{1}{d+1}, \Phi_0(t') \right] dt' \right\} \right) \\ &= 2 \binom{d}{1} |H|^{-1} |m_{\text{st},0}| \left\{ -\Phi_0(t) + \frac{z_0}{d} [\Phi_0(t)]^{d/(d+1)} \gamma \left[\frac{1}{d+1}, \Phi_0(t) \right] \right. \\ &\quad \left. + \frac{z_0}{d+1} \sum_{k=0}^{d-1} \binom{d-1}{k} (-1)^{d-k} [\Phi_0(t)]^{k/(d+1)} \mathcal{A} \left(\frac{-(k+1)}{d+1}, \frac{1}{d+1}, \Phi_0(t) \right) \right\}. \quad (\text{A10}) \end{aligned}$$

It is somewhat easier to evaluate $\Phi_I(t)$. From Eq. (42) and Eq. (A6),

$$\begin{aligned}
\Phi_I(t) &= \lambda(H)I_0\Omega v_0^d \int_0^t m_0(t')(t-t')^d dt' \\
&\approx \lambda(H) \frac{(d+1)\ln(z_0)}{\tau_0^{d+1}} |m_{\text{st},0}| \left\{ - \int_0^t (t-t')^d dt' \right. \\
&\quad \left. + z_0 \int_0^t \exp \left[-\ln(z_0) \left(\frac{t'}{\tau_0} \right)^{d+1} \right] (t-t')^d dt' \right\} \\
&= \lambda(H) |m_{\text{st},0}| \left\{ -\Phi_0(t) + \frac{z_0(d+1)\ln(z_0)}{\tau_0^{d+1}} \right. \\
&\quad \left. \times \int_0^t \sum_{k=0}^d \binom{d}{k} t^k (-t')^{d-k} \exp \left[-\ln(z_0) \left(\frac{t'}{\tau_0} \right)^{d+1} \right] dt' \right\} \\
&= \lambda(H) |m_{\text{st},0}| \left(z_0 \left\{ \sum_{k=0}^d \binom{d}{k} (-1)^{d-k} [\Phi_0(t)]^{k/(d+1)} \int_0^{\Phi_0(t)} x^{-k/(d+1)} e^{-x} dx \right\} \right. \\
&\quad \left. - \Phi_0(t) \right) \\
&= \lambda(H) |m_{\text{st},0}| \left(z_0 \left\{ \sum_{k=0}^d \binom{d}{k} (-1)^{d-k} [\Phi_0(t)]^{k/(d+1)} \gamma \left(1 - \frac{k}{d+1}, \Phi_0(t) \right) \right\} \right. \\
&\quad \left. - \Phi_0(t) \right). \tag{A11}
\end{aligned}$$

Combining Eq. (A10), Eq. (A11), and Eq. (48) gives $m_1(t)$.

REFERENCES

- ¹ D. H. Tarling, *Palaeomagnetism: Principles and Applications in Geology, Geophysics and Archaeology* (Chapman and Hall, New York, 1983).
- ² E. Köster and T. C. Arnoldussen, in *Magnetic Recording*, edited by C. D. Mee and E. D. Daniel (McGraw-Hill, New York, 1987), Vol. 1, p. 98.
- ³ E. F. Kneller and F. E. Luborsky, *J. Appl. Phys.* **34**, 656 (1963).
- ⁴ Y. Martin and H. K. Wickramasinghe, *Appl. Phys. Lett.* **50**, 1455 (1987).
- ⁵ T. Chang, J.-G. Zhu, and J. H. Judy, *J. Appl. Phys.* **73**, 6716 (1993).
- ⁶ M. Lederman, G. A. Gibson, and S. Schultz, *J. Appl. Phys.* **73**, 6961 (1993).
- ⁷ M. Lederman, D. R. Fredkin, R. O'Barr, and S. Schultz, *J. Appl. Phys.* **75**, 6217 (1994).
- ⁸ M. Lederman, S. Schultz, and M. Ozaki, *Phys. Rev. Lett.* **73**, 1986 (1994).
- ⁹ C. Salling, S. Schultz, I. McFadyen, and M. Ozaki, *IEEE Trans. Magn.* **27**, 5184 (1991).
- ¹⁰ L. Néel, *Ann. Géophys.* **5**, 99 (1949).
- ¹¹ W. F. Brown, *J. Appl. Phys.* **30**, 130S (1959); *Phys. Rev.* **130**, 1677 (1963).
- ¹² I. S. Jacobs and C. P. Bean, in *Magnetism*, edited by G. T. Rado and H. Suhl (Academic, New York, 1963), Vol. 3, p. 271.
- ¹³ E. Kneller, in *Magnetism and Metallurgy*, edited by A. E. Berkowitz and E. Kneller (Academic, New York, 1969), Vol. 1.
- ¹⁴ H. Orihara and Y. Ishibashi, *J. Phys. Soc. Jpn.* **61**, 1919 (1992).
- ¹⁵ H. Tomita and S. Miyashita, *Phys. Rev. B* **46**, 8886 (1992).
- ¹⁶ P. A. Rikvold, H. Tomita, S. Miyashita, and S. W. Sides, *Phys. Rev. E* **49**, 5080 (1994).
- ¹⁷ P. A. Rikvold and B. M. Gorman, in *Annual Reviews of Computational Physics I*, edited by D. Stauffer (World Scientific, Singapore, 1994), p. 149, and references therein.
- ¹⁸ R. Carey and E. D. Isaac, *Magnetic Domains and Techniques for their Observation* (Academic Press, New York, 1966).
- ¹⁹ C. Kittel, *Phys. Rev.* **70**, 965 (1946).
- ²⁰ R. Czech and J. Villain, *J. Phys.: Cond. Matter* **1**, 619 (1989).
- ²¹ B. Kaplan and G. A. Gehring, *J. Magn. Magn. Mater.* **128**, 111 (1993).
- ²² A. B. MacIsaac, J. P. Whitehead, M. C. Robinson, and K. De'Bell, *Phys. Rev. B* **51**, 16033 (1995).
- ²³ I. Booth, A. B. MacIsaac, J. P. Whitehead, and K. De'Bell, *Phys. Rev. Lett.* **75**, 950 (1995).
- ²⁴ K.-O. Ng and D. Vanderbilt, *Phys. Rev. B* **52**, 2177 (1995).
- ²⁵ W. F. Brown, *Micromagnetics* (Wiley, New York, 1963).
- ²⁶ A. Lyberatos, D. V. Berkov, and R. W. Chantrell, *J. Phys.: Cond. Matter* **5**, 8911 (1993).
- ²⁷ R. D. Kirby, J. X. Shen, R. J. Hardy, and D. J. Sellmyer, *Phys. Rev. B* **49**, 10810 (1994).
- ²⁸ U. Nowak and A. Hucht, *J. Appl. Phys.* **76**, (1995).
- ²⁹ S. T. Chui and D.-C. Tian, *J. Appl. Phys.* **78**, 3965 (1995).
- ³⁰ H. M. Duiker and P. D. Beale, *Phys. Rev. B* **41**, 490 (1990).
- ³¹ P. D. Beale, *Integrated Ferroelectrics* **4**, 107 (1994).
- ³² H.-B. Braun, *Phys. Rev. Lett.* **71**, 3557 (1993); *J. Appl. Phys.* **75**, 4609 (1994); *Phys. Rev. B* **50**, 16485 (1994); **50**, 16501 (1994).
- ³³ H. L. Richards, S. W. Sides, M. A. Novotny, and P. A. Rikvold, *J. Magn. Magn. Mater.* **150**, 37 (1995).

- ³⁴ H. L. Richards, S. W. Sides, M. A. Novotny, and P. A. Rikvold, J. Appl. Phys. (to be published).
- ³⁵ A. N. Kolmogorov, Bull. Acad. Sci. USSR, Mat. Ser. **1**, 355 (1937).
- ³⁶ W. A. Johnson and P. A. Mehl, Trans. Am. Inst. Mineral Mining Eng. **135**, 365 (1939).
- ³⁷ M. Avrami, J. Chem. Phys. **7**, 1103 (1939); **8**, 212 (1940); **9**, 177 (1941).
- ³⁸ L. Onsager, Phys. Rev. **65**, 117 (1944).
- ³⁹ C. N. Yang, Phys. Rev. **85**, 809 (1952).
- ⁴⁰ P. A. Martin, J. Stat. Phys. **16**, 149 (1977).
- ⁴¹ P. C. Hohenberg and B. Halperin, *Rev. Mod. Phys.* **49**, 435 (1977).
- ⁴² N. Metropolis *et al.*, J. Chem. Phys. **21**, 1087 (1953).
- ⁴³ A. B. Bortz, M. H. Kalos, and J. L. Lebowitz, J. Comp. Phys. **17**, 10 (1975).
- ⁴⁴ M. A. Novotny, Computers in Physics **9**, 46 (1995).
- ⁴⁵ D. Stauffer, Int. J. Mod. Phys. C **3**, 1059 (1992).
- ⁴⁶ L. S. Schulman, J. Phys. A **13**, 237 (1980).
- ⁴⁷ L. S. Schulman, in *Finite Size Scaling and Numerical Simulation of Statistical Systems*, edited by V. Privman (World Scientific, Singapore, 1990), p. 490.
- ⁴⁸ J. Lee, M. A. Novotny, and P. A. Rikvold, Phys. Rev. E **52**, 359 (1995).
- ⁴⁹ C. P. Bean and J. D. Livingston, J. Appl. Phys. **30**, 120S (1959).
- ⁵⁰ C. Domb, in *Phase Transitions and Critical Phenomena*, edited by C. Domb and J. L. Lebowitz (Academic, New York, 1974), Vol. 3.
- ⁵¹ H. Furukawa and K. Binder, Phys. Rev. B **26**, 556 (1982).
- ⁵² C. Rottman and M. W. Wortis, Phys. Rev. B **24**, 6274 (1981).
- ⁵³ R. K. P. Zia and J. E. Avron, Phys. Rev. B **25**, 2042 (1982).
- ⁵⁴ K. Leung and R. K. P. Zia, J. Phys. A **23**, 4593 (1990).
- ⁵⁵ K. Binder, Z. Phys. B **43**, 119 (1981).
- ⁵⁶ K. Binder, Phys. Rev. A **25**, 1699 (1982).
- ⁵⁷ B. Berg, U. Hansmann, and T. Neuhaus, Z. Phys. B **90**, 229 (1993).
- ⁵⁸ I. M. Lifshitz, Sov. Phys. JETP **15**, 939 (1962).
- ⁵⁹ S. K. Chan, J. Chem. Phys. **67**, 5755 (1977).
- ⁶⁰ S. M. Allen and J. W. Cahn, Acta Metall. **27**, 1085 (1979).
- ⁶¹ J. A. N. Philipe, A. J. Bray, and S. Puri, (submitted to Phys. Rev. E) (unpublished).
- ⁶² R. A. Ramos, S. W. Sides, P. A. Rikvold, and M. A. Novotny, in preparation (unpublished).
- ⁶³ K. Sekimoto, Physica A **135**, 328 (1986).
- ⁶⁴ D. L. Mills, in *Ultrathin Magnetic Structures*, edited by J. A. C. Bland and B. Heinrich (Springer-Verlag, New York, 1994), Vol. 1.

FIGURES

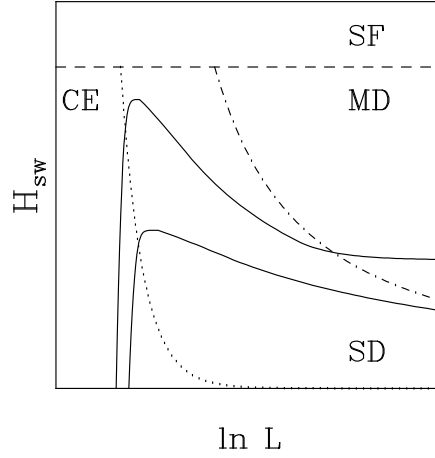


FIG. 1. The relationship between the applied field H and system width L for a shorter (top solid curve) and a longer (bottom solid curve) fixed lifetime in a typical metastable magnetic system. Four regions are distinguished by differing decay processes: the Coexistence region (CE), the Single-Droplet region (SD), the Multi-Droplet region (MD), and the Strong-Field region (SF). The CE and SD regions are separated by the thermodynamic spinodal (dotted curve). The SD and MD regions are separated by the dynamic spinodal (dash-dotted curve). The SF region is separated from the other regions by the mean-field spinodal (dashed curve). [Reproduced from Fig. 1 of Ref. 33.]

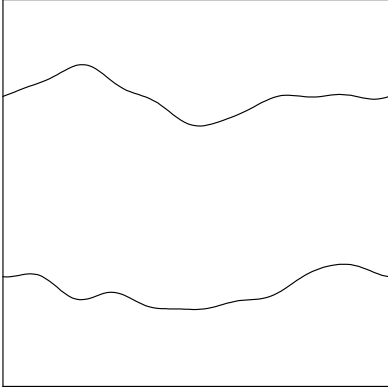


FIG. 2. Configurations that may occur during the reversal process. As in the text, periodic boundary conditions are imposed. (a) A sketch of a “slab” configuration. (b) A typical realization of a single droplet in the process of overtaking the system. Grey squares are “up” spins and black squares are “down” spins. Here $L=60$, $H=-0.08J$, $D=0$, $T=0.8T_c$, and $t=410$ MCSS. [Figure courtesy S. W. Sides.] (c) A typical realization showing the nucleation and growth of several droplets in the process of switching the magnetization. Here $L=120$, $H=-0.2J$, $D=0$, $T=0.8T_c$, and $t=114$ MCSS. [Reproduced from Fig. 5(b) of Ref. 33.]

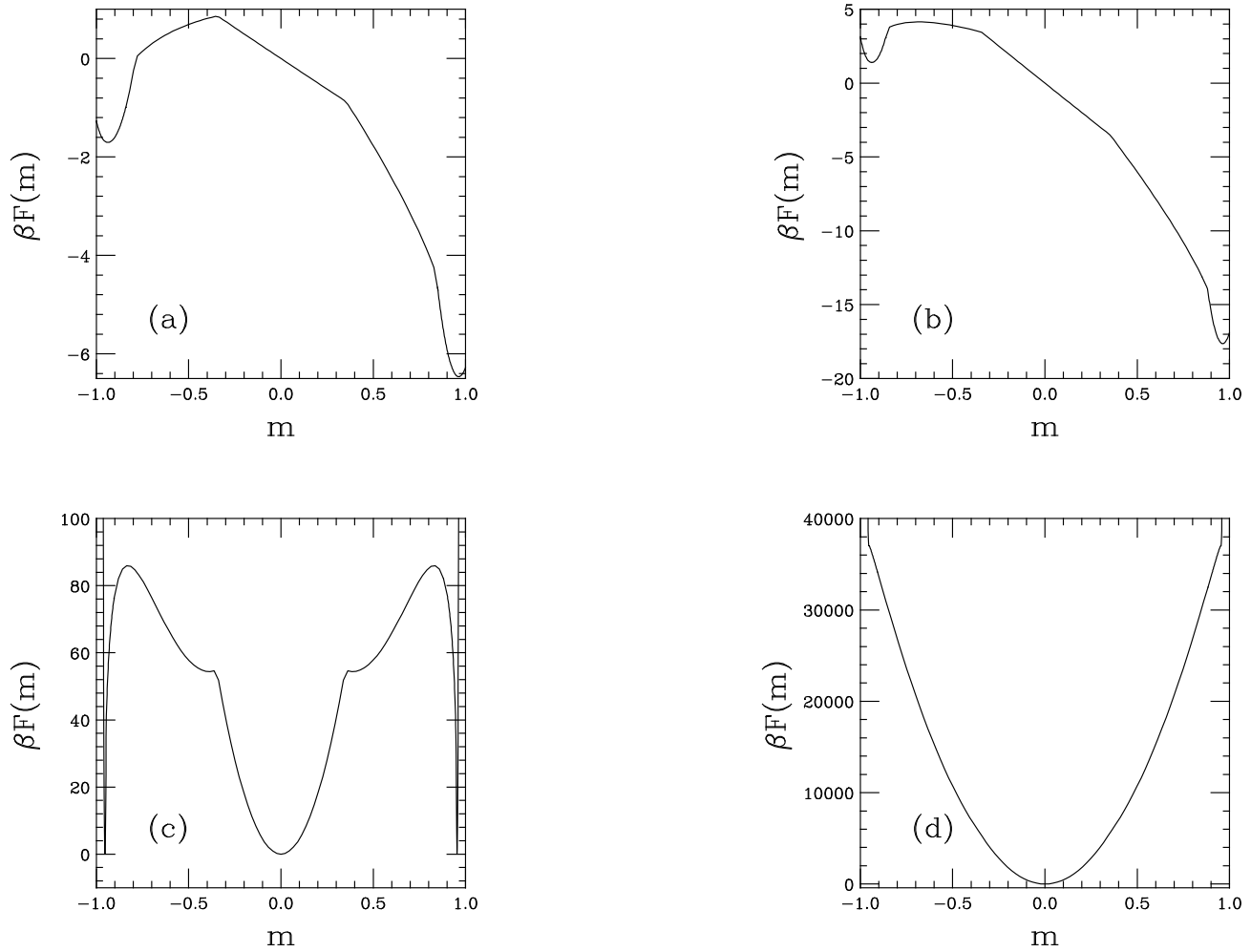


FIG. 3. The approximate restricted free energy function $F(m)$ as determined by Eq. (9) with $d=2$, $T=0.8T_c$, and $L_D=500$. (a) $L=5$, $H=0.1J$. (b) $L=10$, $H=0.1J$. (c) $L=500$, $H=0$. (d) $L=5000$, $H=0$.

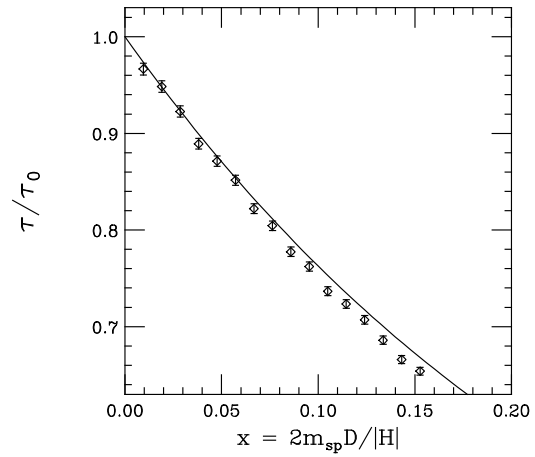


FIG. 4. The relative lifetime *vs.* $x = 2m_{sp}D/|H|$ in the SD region as given by Eq. (27). $|H|=0.2J$, $T=0.8T_c$, and $L=10$. Each Monte Carlo point represents 47 500 decays. The quantity Ξ_1 was obtained in Ref. 33 from data at $D=0$ and is *not* the result of a fit to the D -dependence.

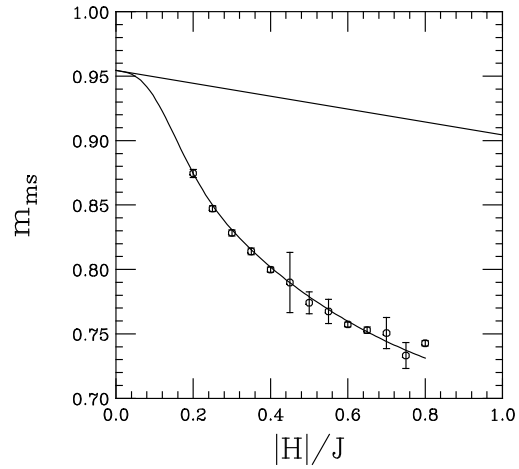


FIG. 5. The metastable magnetization *vs.* H in the MD region. The data points were estimated by Ramos *et al.*⁶² by extrapolating back to $t=0$ assuming Avrami's Law. The smooth curve is a useful estimate, but the correct form of m_{ms} *vs.* H is not known except near $H=0$, where Eq. (11b) applies. The straight line indicates the approximation Eq. (11b).

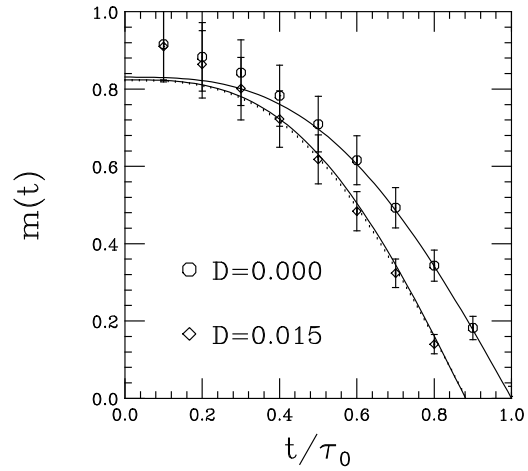


FIG. 6. The magnetization *vs.* time in the MD region as given by Eq. (34) and Eq. (48). $H=0.3J$, $T=0.8T_c$, and $L=50$. The two values of D displayed are $D=0$ and $D=0.015$. The solid curves are $m_0(t) + Dm_1(t)$; the dotted curve (hardly distinguishable on the scale of this figure) is $m_f(t)$. Each Monte Carlo point represents 100 decays.

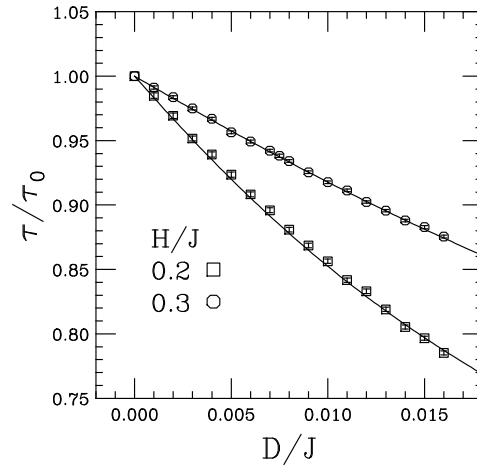


FIG. 7. The lifetime *vs.* D in the MD region for $T=0.8T_c$ with $H=0.2J$ and $H=0.3J$. The solid curves represent the theoretical predictions given by combining Eq. (50) and Eq. (51) and are *not* the result of a fit to the D -dependence. Each Monte Carlo point represents at least 5 000 decays in a system of size $L=100$. [Reproduced from Fig. 4 of Ref. 34.]